

MiR-24 alleviates cardiomyocyte apoptosis after myocardial infarction via targeting BIM

L.-J. PAN, X. WANG, Y. LING, H. GONG

Division of Cardiology, Department of Medicine, Jinshan Hospital, Fudan University, Shanghai, China

Abstract. – **OBJECTIVE:** Ischemia hypoxia induces cardiomyocyte (CM) apoptosis in the process of acute myocardial infarction (AMI). It was showed that pro-apoptosis factor BIM participates in regulating tumor cell apoptosis under ischemia or hypoxia condition, while its role in CM apoptosis after AMI is still unclear. It was revealed that miR-24 expression was significantly reduced in myocardial tissue after AMI. Bioinformatics analysis exhibits that miR-24 is targeted to the 3'-UTR of BIM. This study aims to investigate the role of miR-24 in mediating BIM expression and CM apoptosis.

PATIENTS AND METHODS: Dual-luciferase assay was used to confirm the targeted regulation between miR-24 and BIM. Cells were cultured under ischemia hypoxia for 12 h after transfection for 48 h. Cell apoptosis was tested by using flow cytometry. The caspase activity was detected by using fluorescence spectrophotometry. Wistar rats were divided into four groups, including Sham, AMI, AMI+agomir control, and AMI + agomir-24 groups. Cardiac function was evaluated by using echocardiography. CM apoptosis was determined by using TUNEL staining. Infarction area was measured by using Masson's trichrome staining. MiR-24 targeted suppressed BIM expression.

RESULTS: MiR-24 miRNA and/or BIM transfection significantly declined BIM levels, inhibited caspase-9 and caspase-3 activities, and reduced cell apoptosis in H9C2 cells. MiR-24 expression was decreased while BIM levels were up-regulated in myocardium after AMI. Agomir injection down-regulated the BIM expression in myocardium, reduced CM apoptosis, reduced infarction area, and improved cardiac function in rats.

CONCLUSIONS: MiR-24 was reduced, whereas BIM was enhanced in the CM after AMI. MiR-24 up-regulation plays a critical role in decreasing BIM expression, reducing CM apoptosis, and improving cardiac function after AMI.

Keywords: miR-24, BIM, acute myocardial infarction, Cardiomyocyte, Apoptosis.

Introduction

Acute myocardial infarction (AMI) refers to the myocardial necrosis induced by coronary ar-

tery acute and persistent ischemic hypoxia. AMI mainly exhibits severe and sustained retrosternal pain, clinical complications with cardiac arrhythmia, shock, and heart failure. The AMI is also one of the most important causes of cardiac death. Cardiomyocyte (CM) ischemia hypoxia in the process of myocardial infarction can cause CM irreversible death or apoptosis, resulting in cardiac insufficiency³. CM apoptosis and necrosis caused by myocardial ischemia hypoxia may induce ventricular remodeling, deteriorating cardiac function, and forming continuous cardiac dysfunction⁴. Particular factors in CM always induce disorders after ischemia and hypoxia. Regulation of related factors expression may reduce cell apoptosis, thus to provide new methods for treating myocardial infarction and improving myocardial function. Bcl-2 interacting mediator of cell death (BIM), also known as the Bcl-2-like protein 11 (BCL2L11), belongs to the subfamily member of Bcl-2 family containing BH3-only structural domain^{5,6}. As a kind of important apoptosis regulatory protein, BIM widely distributes in a variety of tissues and cells. It is closely related to promoting cell apoptosis⁷. It was showed that BIM participates in tumor cell apoptosis under ischemia⁸ or hypoxia^{9,10}. However, the role of BIM in regulating CM apoptosis after AMI still needs to be investigated. MiRNAs are a type of endogenous single strand non-coding RNA at the length of 22-25 nucleotides. The miRNAs can negatively regulate target gene expression via complete or incomplete complementary binding with 3'-untranslated region (3'-UTR) to degrade mRNA or block mRNA translation at posttranscriptional level¹¹. More and more evidence suggested that the abnormal expression and dysfunctions of miRNAs were involved in cardiac remodeling after myocardial infarction¹². The results indicated that the miR-24 was significantly decreased in myocardium after infarction¹³. Bioinformatics analysis showed the complementary binding site between miR-24 and the 3'-UTR of BIM mRNA. This work explored

the role of miR-24 in regulating BIM expression and affecting CM apoptosis.

Materials and Methods

Main reagents and materials

Healthy male Wistar rats at 8-10 weeks and weighted 220-250 g were purchased from Shanghai Fudan University, Shanghai, China. Rat myocardial cell line H9C2 was got from Shanghai Cell Bank of Chinese Academy of Sciences. Cell culture reagents were bought from Gibco (Grand Island, NY, USA). RNA extraction reagent Trizol was purchased from Invitrogen Life Technologies (Carlsbad, CA, USA); reverse transcription and Real-time PCR kits were from TaKaRa (Dalian, China); micRON™ agomir-24, micRON™ agomir-control, miR-24 mimic, miR-24 inhibitor, and negative control were designed and synthesized by RiboBio (Guangzhou, China). Rabbit anti-BIM and β -actin antibodies were obtained from Abcam (Cambridge, MA, USA). Caspase-3 and caspase-9 activities detection kits, and TUNEL apoptosis detection kit were bought from Beyotime (Shanghai, China). Horseradish peroxidase (HRP) labeled goat anti rabbit secondary antibody was purchased from Jackson Immuno Research (West Grove, PA, USA). Dual-luciferase® reporter assay system and luciferase-3-promoter plasmid was bought from Promega (Madison, WI, USA).

Rat AMI modeling and sample collection

Wistar rats were kept in a clean environment with standard feeding and free drinking. The diurnal cycle was 12h light/12h dark, humidity was 60%, and room temperature was between 20°C and 22°C. The padding was changed twice a week, while the basket was cleaned twice a week. The rat was anesthetized by using 10% chloral hydrate intraperitoneal injection at 5 mg/g. Electrocardiogram was connected for monitoring. The neck was dissected, separate trachea. Then, the trachea was intubated and connected to animal breathing machine with breathing ratio at 1:2, breathing frequency at 60 times/min, and tidal volume at 10-12 mL. The chest was opened by the left intercostal and the pericardium was opened to expose the heart. Next, the anterior descending branch was identified and ligated by 6-0 non-traumatic sutures. ECG monitor exhibited ST segment arch lift for 0.1 mV or T wave high, pale myocardium, and

abate pulse were applied to confirm the AMI model success. The Wistar rats were randomly equally divided into four groups with 15 in each group. The rats in sham group received anterior descending branch ligation. The rats in AMI group were modeled as AMI. The rats in AMI + agomir-control received 2×10^3 mol/L agomir-control local injection at 24 h before AMI modeling. Five points were selected on the surface of myocardium, with 10 μ l injection in each point. The rats in AMI + agomir-24 received 2×10^3 mol/L agomir-24 local injection at 24 h before AMI modeling. Five points were selected on the surface of myocardium, with 10 μ l injection in each point. The usage of all experimental animals was strictly abided by the Jinshan Hospital, Fudan University Animal Management Committee Regulation Ordinance and approved by Jinshan Hospital, Fudan University experimental Animal Ethics Committee.

Echocardiography

The rats in each group were anesthetized by 10% chloral hydrate (Sigma-Aldrich, St. Louis, MI, USA) intraperitoneal injection at 1 week after AMI modeling to perform echocardiography. Left ventricular end diastolic diameter and left ventricular end systolic diameter and left ventricular end diastolic diameter were recorded at the level of papillary muscle prior to mitral valve through the left ventricular short axis view. Left ventricular ejection fraction (LVEF) and left ventricular fractional shortening (LVFS) were automatically calculated.

Rat myocardium sample preparation

The tissue samples at MI region were extracted from rats at 1 week after modeling and used for RNA and protein extraction, and frozen section.

TUNEL assay

Myocardium sample was extracted from the rats at 1 week after modeling to prepare frozen section. TUNEL detection kit was used to measure cell apoptosis (Sigma-Aldrich, St. Louis, MI, USA). The section was fixed in 4% paraformaldehyde (Sigma-Aldrich) for 60 min and washed by phosphate-buffered saline (PBS) for twice. Next, the section was treated by using 0.15 Triton X-100 on ice for 2 min and was added with 50 μ l TUNEL detection fluid prepared by TdT enzyme and fluorescence label liquid at 37°C for 60 min. At last, the section was tested under 488 nm to analyze cell apoptosis.

Myocardial infarction area measurement

The rats received 1 ml 2% Evans blue intravenous injection at 1 week after modeling. Then the left ventricular wall tissue was extracted and cut into slice at 3 mm. Next, the slice was incubated in 2% TTC at 37°C for 15 min. After washed by normal saline and fixed by 4% paraformaldehyde, the slice was observed under the microscope. The infarcted myocardium exhibited as grey white, while the non-infarcted myocardium presented as brick red. Myocardium infarction area = infarction area/(infarction area + non-infarction area) × 100%.

Rat CM cell transfection and ischemia hypoxia treatment

Rat CM cells H9C2 were cultured in Dulbecco's Modified Eagle Medium (DMEM) (Gibco, Grand Island, NY, USA) containing 10% FBS (Gibco) and maintained in 37°C and 5% CO₂. Cells in logarithmic phase were divided into five groups, including mimic NC, miR-24 mimic, si-NC, si-BIM, and miR-24 mimic + si-BIM. After 48 h, the cells were incubated in low-glucose DMEM medium without FBS to simulate ischemia environment, and then cultured in ischemia hypoxia environment with 1% O₂, 5% CO₂, and 94% N₂ to simulate hypoxia for 12 h.

Luciferase reporter gene vector construction

The 3'-UTR of BIM gene was amplified based on HEK293 cell genome. PCR product was recycled and connected to pGL3-M2 vector. DH5α competent cells (Takara, Dalian, China). After colony PCR, the positive clone was screened and the plasmid with correct sequence was applied for cell transfection.

Luciferase reporter gene assay

The HEK293 cells were transfected with 500 ng pGL3-M2-3'UTR, 30 nmol miR-24 nucleotide fragment, and 80 ng pRL-TK mixture mediated by Lipofectamine 2000 (Invitrogen Technologies). After incubated for 6 h, DMEM medium was changed to DMEM medium supplemented with 10% FBS and 1% penicillin-streptomycin for another 48 h. Luciferase activity was detected according to the manual provided by the kit (Invitrogen Life Technologies). After washed by PBS for twice, the cells were added with 100 μl PLB for 30 min at room temperature and centrifuged at 1,000 ×g for 10 min. The supernatant was added with 100

μl LAR II and tested immediately in chemiluminescence apparatus for fluorescence I. Then the solution was added with 100 μl Stop&Glo solution to test fluorescence II. The fluorescence I and II was treated as relative expression level of luciferase activity.

qRT-PCR

The reverse transcription system contained 2 μg total RNA, 0.75 μL dNTP at 10 mmol/L, RT Buffer (5×), 1.2 μL RT primer (1 μmol/L), 2 μL reverse transcriptase, 5 μL RNase inhibitor, and ddH₂O. The reaction was performed at 16°C for 30 min, 42°C for 15 min, 85°C for 5 min. The PCR primers used were as follows: miR-24P_F: 5'-TCACAGCACTACATTGCCAG-3', miR-24P_R: 5'-TCTGGTCTCTGCTCTCTGTCTC-3'; U6P_F: 5'-ATTGGAACCTACAGAGAAGATT-3', U6P_R: 5'-GGAACCTCACGAATTTG-3'; β-actinP_F: 5'-TAAGTTCTGAATGTGACCGAGA-3', β-actinP_R: 5'-GCTCTGTCTGTAGGGAGGTAGG-3'; β-actinP_F: 5'-GACCTTAAGGCCAAC-3', β-actinP_R: 5'-TGTCACACGATTTCC-3'. The PCR reaction system (Invitrogen Life Technologies) was composed of 4.5 μl 2×SYBR Green Mixture, 0.5 μl forward and reverse primer at 5 μM, 1 μl template and 3.5 μl ddH₂O. The reaction was performed on ABI ViiA7 at 95°C for 5 min, followed by 40 cycles of 95°C for 15 s and 60°C for 60 s. Comparative Ct method (2^{-ΔΔCT}) was applied for data analysis. U6 and β-actin were selected as housekeeping control. Each test was repeated for 3 times.

Western blot

Total protein was extracted from the cells and quantified by bicinchoninic acid assay (BCA) method. A total of 50 μg protein was separated by sodium dodecyl sulphate-polyacrylamide gel electrophoresis (SDS-PAGE) and transferred to polyvinylidene fluoride (PVDF) membrane (Bio-Rad Laboratories, Hercules, CA, USA). After blocked by 5% skim milk at room temperature for 60 min, the membrane was incubated in primary antibody at 4°C overnight (Santa Cruz Biotechnology, Santa Cruz, CA, USA). After washed by PBST, the membrane was further incubated in HRP labeled secondary antibody (Santa Cruz Biotechnology) at room temperature for 60 min. At last, the membrane was treated by ECL chemiluminescence reagent (Amersham, Piscataway, NJ, USA) and was developed for analysis.

Caspase-3 and caspase-9 activities detection

The standard substrate pNA (10 mM) was diluted to 0, 10, 20, 50, 100, and 200 μM, respectively. Their absorbance at 405 nm was tested to draw the standard curve. The cells were digested and centrifuged at 600 ×g and 4°C for 5 min. After cells were washed by PBS, a total of 2×10⁶ cells were added to 100 μl lysis at 4°C for 15 min. After the supernatant was centrifuged at 18,000 ×g for 10 min, it was moved to a precooled Ep tube. For caspase-3, a total of 10 μl Ac-DEVD-pNA (2 mM) was added to the solution and incubated at 37°C for 120 min to test absorbance at 405 nm. For caspase-9, a total of 10 μl Ac-LEHD-pNA (2 mM) was added to the solution and incubated at 37°C for 2 h to test absorbance at 405 nm.

Flow cytometry

The cells were digested by enzyme and were collected. After, the cells were resuspended in 100 μl binding buffer, and 5 μl Annexin V-FITC and 5 μl propidium iodide (PI) were added at room temperature avoiding of light for 30 min. Then, the cells were tested on flow cytometry (Beckman Coulter, Miami, FL, USA).

Statistical Analysis

SPSS 18.0 software (SPSS Inc., Chicago, IL, USA) was applied for data analysis. Measurement data was presented as mean ± standard deviation and compared by *t*-test. *p*<0.05 was depicted as significant difference.

Results

MiR-24 targeted and regulated BIM expression

Dual luciferase reporter assay exhibited that miR-24 mimic or inhibitor significantly reduced or enhanced the relative luciferase activity in HEK293 cells, respectively, confirming that BIM was the target gene of miR-24 (Figure 1A-C). It suggested that miR-24 can target bind with 3'-UTR of BIM mRNA to regulate its expression.

Ischemia hypoxia intervention induced H9C2 cell apoptosis and down-regulated miR-24 expression

Ischemia hypoxia treatment *in vitro* significantly induced H9C2 cell apoptosis compared with control cultured H9C2 cells (Figure 2A). MiR-24 expression was reduced, while BIM gene expression was markedly enhanced after intervention (Figure 2B-C).

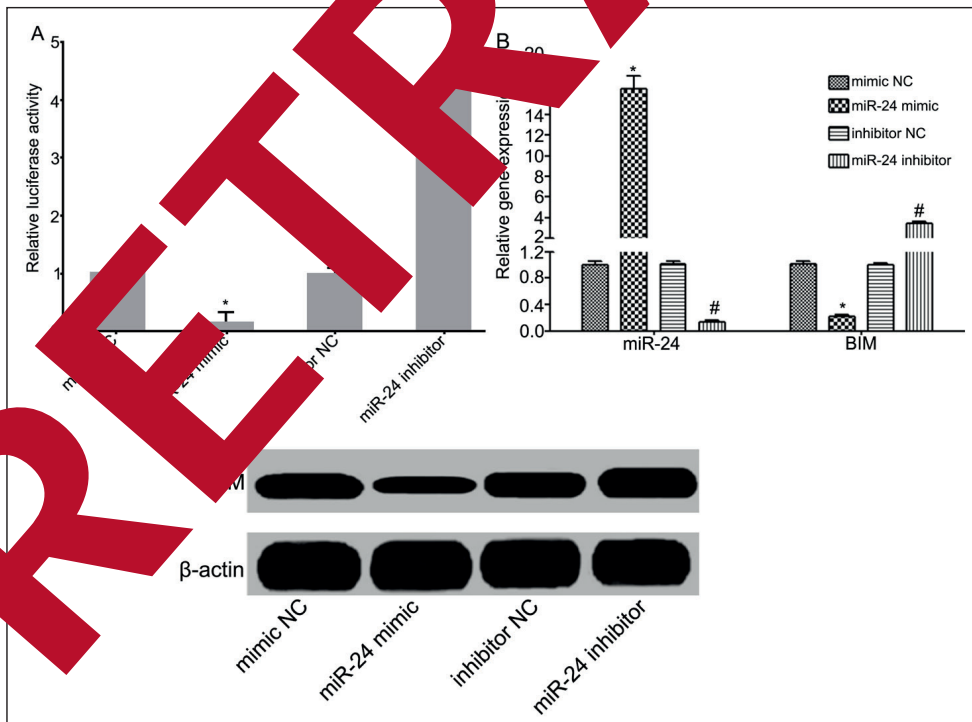


Figure 1. MiR-24 targets and regulates BIM expression. **A**, Dual luciferase reporter assay. **B**, qRT-PCR detection of miR-24 and BIM gene expression. **C**, Western blot detection of BIM protein expression. **p*<0.05, compared with mimic NC. #*p* < 0.05, compared with inhibitor NC.

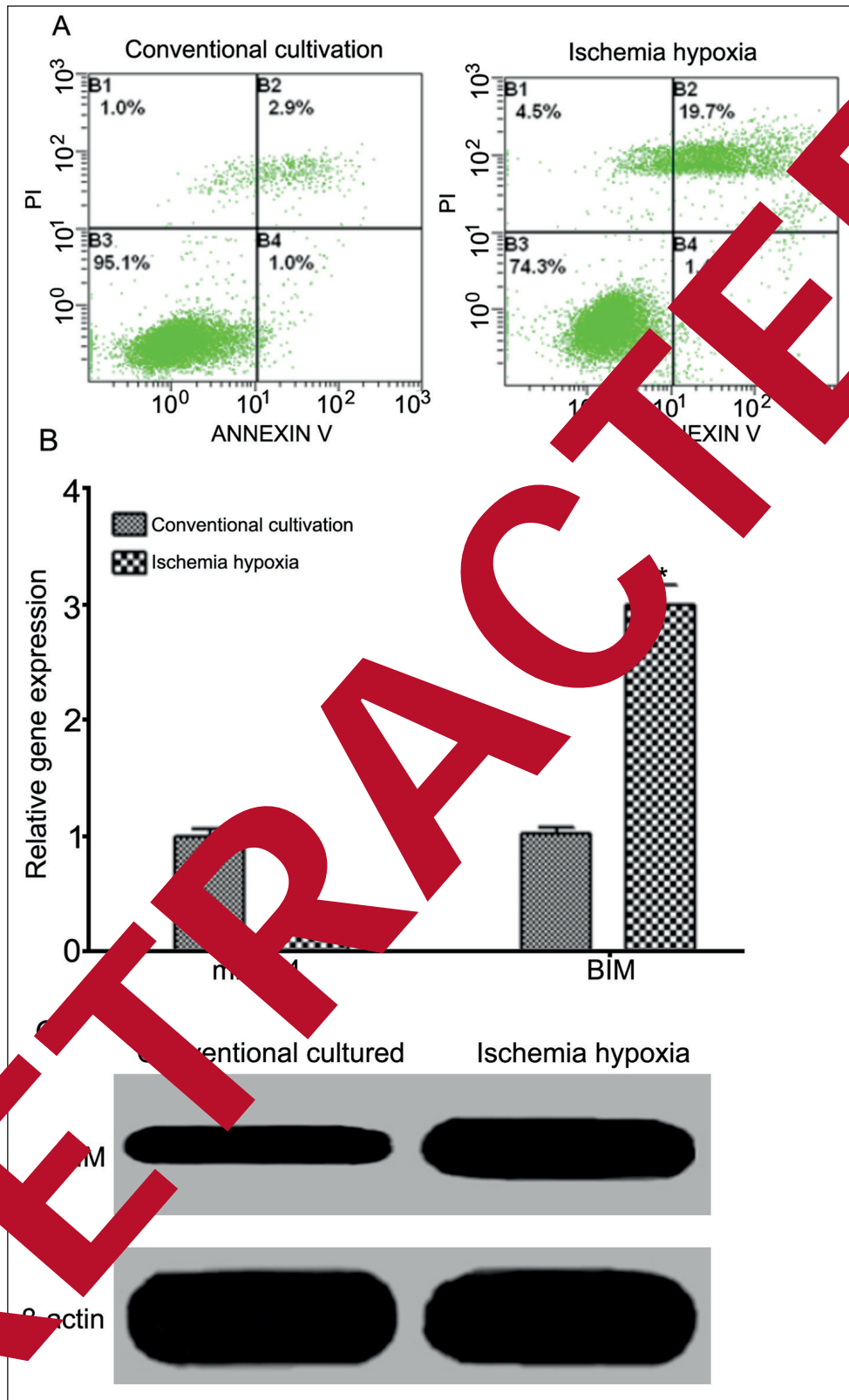


Figure 2. Ischemia hypoxia intervention induces H9C2 cell apoptosis and down-regulates miR-24 expression. **A**, Flow cytometry detection of cell apoptosis. **B**, qRT-PCR detection of miR-24 and BIM gene expression. **C**, Western blot detection of BIM protein expression. * $p < 0.05$, compared with normal cells.

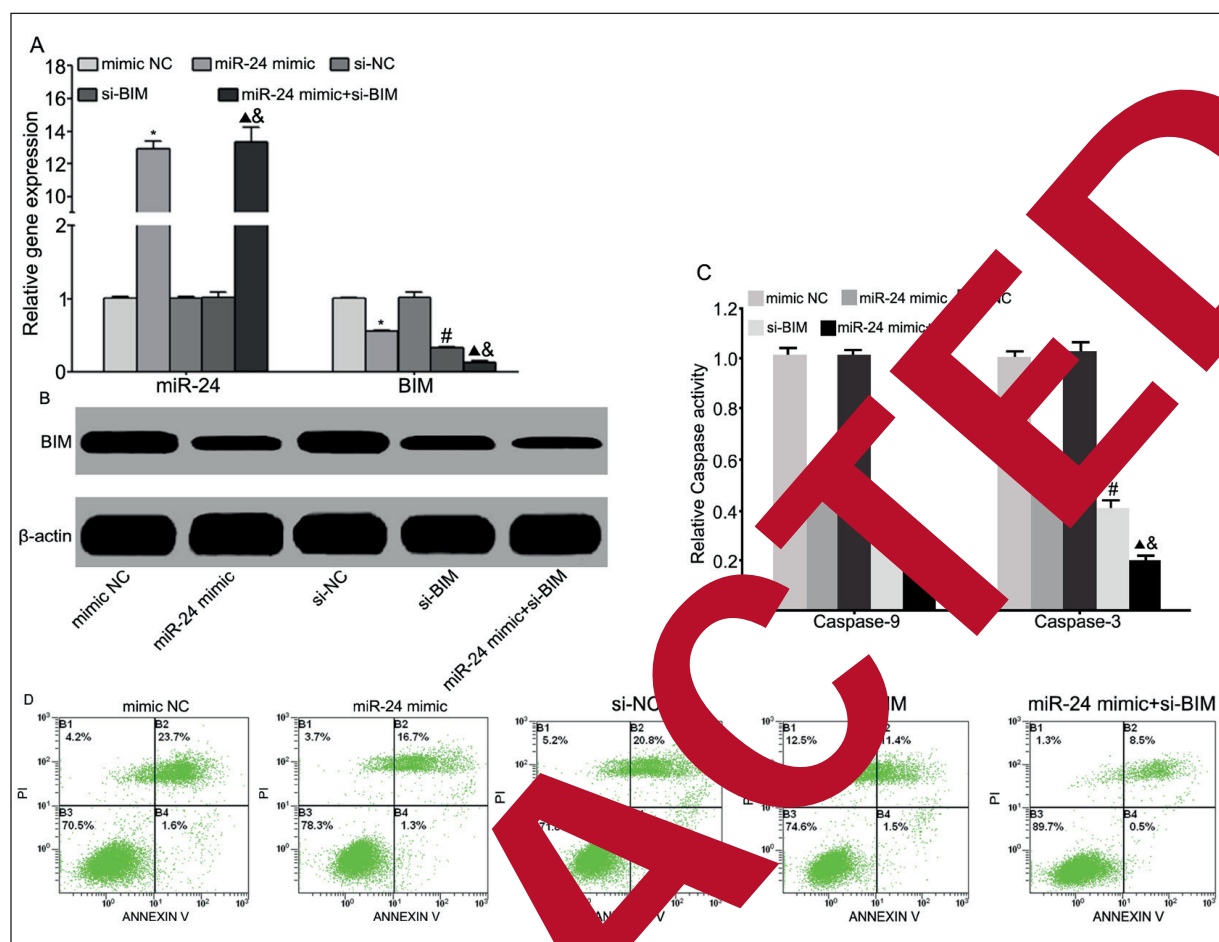


Figure 3. MiR-24 elevation reduces apoptosis induced by ischemia hypoxia. **A**, qRT-PCR detection of gene expression. **B**, Western blot detection of BIM protein expression. **C**, Spectrophotometry detection of caspase activity. **D**, Flow cytometry detection of cell apoptosis. * $p < 0.05$, miR-24 mimic compared with mimic NC. # $p < 0.05$, si-BIM compared with si-NC. $\Delta p < 0.05$, miR-24 mimic + si-BIM compared with mimic NC. & $p < 0.05$, miR-24 mimic + si-BIM compared with si-NC.

MiR-24 elevation reduced H9C2 cell apoptosis induced by ischemia hypoxia

Compared with mimic NC, miR-24 mimic transfection significantly increased BIM expression in H9C2 cells (Figure 3B) and reduced cell apoptosis induced by ischemia hypoxia. Compared with si-NC, BIM silence obviously enhanced apoptosis resistance of H9C2 cell after it was induced by ischemia hypoxia. Caspase-3 and Caspase-9 activity were reduced, whereas apoptosis sensitivity to ischemia hypoxia declined to the low level in H9C2 cells after miR-24 over-expression and BIM silence (Figure 3C-D).

Regulation of miR-24 protected CM apoptosis after AMI

As showed that compared with sham group, LVEF and LVFS markedly decreased (Table I), CM apoptosis significantly elevated (Table II),

infarction area enlarged (Table III), miR-24 apparently reduced, and BIM level enhanced (Figure 4A-B) in AMI group. Compared with agomir-control, agomir-24 intra-myocardial injection improved LVEF and LVFS (Table I), decreased CM apoptosis (Table II), reduced infarction area

Table I. Echocardiographic detection (%; n=10, Mean \pm SD).

Item	Grouping	7 days after modeling
LVEF	Sham	82.5 \pm 4.3
	AMI	65.3 \pm 2.2
	AMI+agomir-control	64.7 \pm 3.1
	AMI+agomir-24	73.5 \pm 2.4
LVFS	Sham	47.7 \pm 3.3
	AMI	35.1 \pm 2.8
	AMI+agomir-control	36.4 \pm 3.0
	AMI+agomir-24	42.6 \pm 2.9

Table II. CM apoptosis comparison (% , n=10, Mean ± SD).

Group	7 days after modeling
Sham	5.5±1.1
AMI	29.5±5.1
AMI+agomir-control	30.7±6.2
AMI+agomir-24	19.6±3.7

Table III. Myocardial infarction area comparison (% , n=10, Mean ± SD).

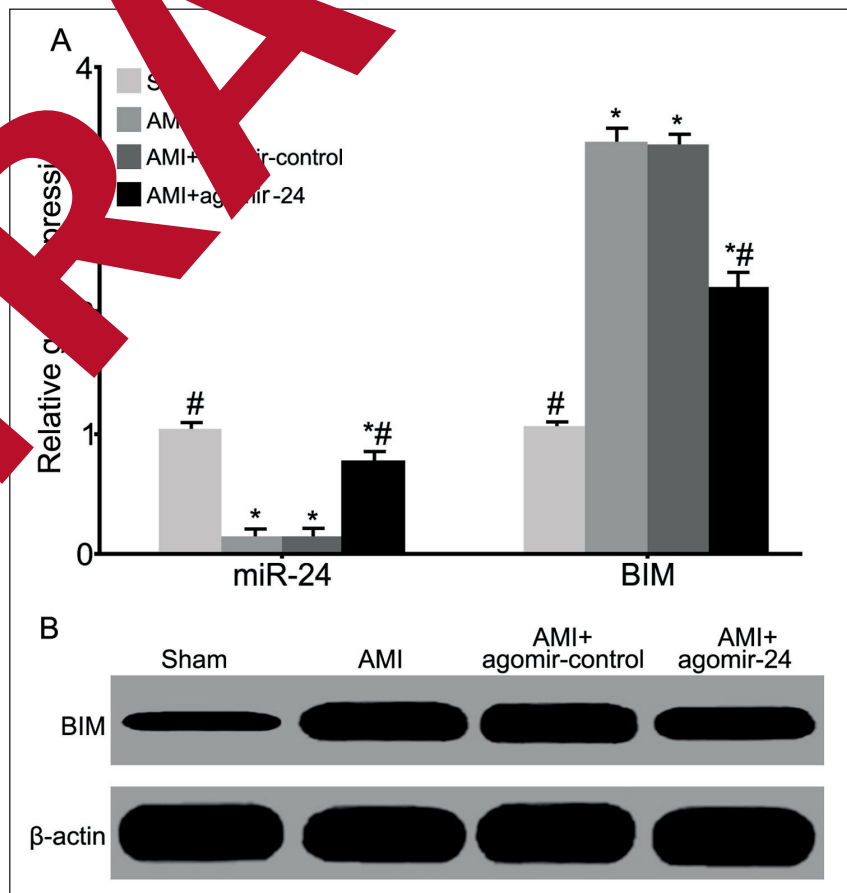
Group	7 days after modeling
Sham	0.0±0.0
AMI	42.7±5.1
AMI+agomir-control	44.5±6.2
AMI+agomir-24	27.2±2.1

(Table III), and declined BIM expression (Figure 4 A-B). It indicated that miR-24 elevation can downregulate BIM expression, reduce CM apoptosis after infarction, narrow infarction area, and improve cardiac function.

Discussion

Myocardial infarction caused by myocardial ischemia anoxic is a type of cardiovascular disease seriously harm to human health and one of the most common causes of heart failure¹⁴. AMI is featured as complicated pathogenesis, critical condition and a rapid progress. It is easy to en-

danger patient's life or cause serious sequelae. If it is not treated in time, at present, there are 10 million people death of cardiovascular disease worldwide every year. More than a half of them died of AMI¹⁶. It was reported that the incidence of AMI in China was 45-55/100,000. Following the aggravation of ageing society, speeding up of modern life rhythm, improvement of living standards, changes in diet and increase of mental pressure, the incidence of AMI exhibits rising trend year by year in our country. Ischemia and hypoxia may cause CM irreversible apoptosis and necrosis, induce ventricular remodeling, deteriorate cardiac function, and form sustainable cardiac dysfunction effect in the process of MI⁴. CM



regulation of miR-24 detected CM apoptosis after AMI. RT-PCR detection of gene expression. **B**, Western blot detection of BIM protein expression. * $p < 0.05$, compared with Sham. # $p < 0.05$, compared with AMI.

apoptosis plays an important role in the pathophysiology process of cardiac dysfunction after infarction, heart failure, and cardiac remodeling. Therefore, reducing CM apoptosis is of great significance in improving myocardial function after infarction and delaying the cardiac remodeling process¹⁸. CM apoptosis and necrosis are one of the major pathological mechanisms of cardiac insufficiency after AMI. Necrosis often occurs in the late phase of ischemia, whereas apoptosis occurs earlier and throughout the entire process. Thus, how to effectively reduce or avoid CM apoptosis after infarction became a hot issue in clinic¹⁹. Particular factors in CM appear to be disorder after ischemia and hypoxia. Regulation of related factors expression may reduce cell apoptosis, thus providing a new thought for treating myocardial infarction and improving myocardial function. BIM, a member of the subfamily of Bcl-2 protein family containing BH3-only domain structure, is the core regulatory protein in mitochondrial apoptosis pathway. It is a key factor in mediating apoptosis in various cell types⁷. The BH3-only domain structure of BIM is the main domain to promote apoptosis, which transfers Bax from cytoplasm to the mitochondria and increases the permeability of mitochondrial membrane. It further leads to cytochrome C-release to cytoplasm, activating caspase-9 and downstream caspase-3, resulting in mitochondrial dependent endogenous apoptosis pathway activation²⁰. It was demonstrated that BIM participated in tumor cell apoptosis under ischemia⁸ or hypoxia^{9,10}. However, the role of regulating CM apoptosis after AMI still needs to be investigated. It was found that miR-24 obviously decreased in myocardium after infarction¹³. Bioinformatics analysis showed the complementary binding site between miR-24 and the 3'-UTR of BIM mRNA. This paper explored the role of miR-24 in regulating BIM expression and affecting CM apoptosis. Dual luciferase reporter assay revealed that miR-24 mimic or inhibitor transfected significantly reduced or enhanced BIM expression in H9C2 cells, suggesting that miR-24 can bind with 3'-UTR of BIM mRNA to regulate its expression. Ischemia hypoxia treatment *in vitro* significantly induced H9C2 cell apoptosis, down-regulated miR-24 expression, and elevated BIM level compared with conventional cultured H9C2 cells, indicating that miR-24 reduction may play a role in increasing BIM expression and promoting CM apoptosis after ischemia hypoxia. Gao et al²¹ reported that

hypoxia obviously up-regulated BIM expression in CM cultured *in vitro* and induced CM apoptosis. Huang et al¹⁰ revealed the role of BIM upregulation in low glucose hypoxia induced cell apoptosis. Our results suggested that ischemia hypoxia up-regulated BIM expression in H9C2 cells and facilitated cell apoptosis, which was in accordance to Gao et al²¹ and Huang et al¹⁰ findings. MiR-24 mimic and/or miR-24 siRNA transfection significantly suppressed BIM expression in H9C2 cells and reduced cell apoptosis induced by ischemia hypoxia. Compared with si-NC, BIM silence obviously enhanced apoptosis resistance of H9C2 cells after it was treated by ischemia hypoxia. Another experiment showed that miR-24 appeared to be down-regulated and BIM level enhanced in AMI group, which was in accordance with *in vitro* results. Liu et al²² demonstrated BIM over-expressed in myocardium from hypoxia infarction in animal experiment, which was similar with our results. Sholamin et al²³ indicated that compared with control, miR-24 expression in peripheral blood from AMI patients was apparently reduced. Moreover, miR-24 elevation down-regulated BIM expression, reduced CM apoptosis after infarction, narrowed infarction area, and improved cardiac function. Izarra et al²⁴ showed that over-expression of miR-133a reduced BIM expression in cardiac progenitor cells (CPCs) and promoted transplanted CPCs proliferation and survival in the heart tissue from rat MI model to improve cardiac function and reduce the myocardial fibrosis after myocardial infarction. It suggested the protecting and treatment effect of reducing BIM in infarcted myocardium. Bhuiyan et al²⁵ presented that as a kind of myocardial protective drug, vanadyl sulfate can reduce BIM level and increase FLIP expression in CM, and inhibit caspase-3 and caspase-9 activities through activating AKT signaling pathway. Our results revealed the role of down-regulating BIM in protecting CM from apoptosis after infarction and improving heart function, which was similar to Izarra et al²⁴ study. Hu et al²⁶ reported that over-expression of miR-21, miR-24, and miR-221 enhanced CPCs resistance to serum starvation, prolonged transplanted CPCs survival in rat AMI model, and improved cardiac function. Guo et al²⁷ discovered that compared with wild type mice, myh6-miR-24 transgenic mice appeared sensitivity reduction to AMI, presenting as declined CM apoptosis after AMI, narrowed infarction area, and improved cardiac function. In addition to CM protection, Wang et al¹³ showed over-expres-

sion of miR-24 can significantly reduce secretion of TGF- β and phosphorylation of Smad 2/3 in cardiac fibroblasts to improve cardiac function after AMI.

Conclusions

MiR-24 was reduced, whereas BIM was enhanced in CM after AMI. MiR-24 up-regulation plays a critical role in decreasing BIM expression, reducing CM apoptosis, and improving cardiac function after AMI.

Conflict of Interests

The Authors declare that they have no conflict of interests.

References

- LISOWSKA A, MAKAREWICZ-WUJEC M, FILIPIAK KJ. Risk factors, prognosis and secondary prevention of myocardial infarction in young adults in Poland. *Kardiol Pol* 2016; 74: 1148-1153.
- DAVIES N. Treating ST-elevation myocardial infarction. *Emerg Nurse* 2016; 24: 20-25.
- STELTER Z, STRAKOVA J, YELLAMILI A, FISCHER K, TROPPE K, TOWNSEND D. Hypoxia-induced cardiac injury in dystrophic mice. *Am J Physiol Heart Circ Physiol* 2016; 310: H938-H948.
- LI R, GENG HH, XIAO J, QIN Y, LIU Y, LIU X, XING JM, XIA YF, MAO Y, LIANG JW, JI Y. miR-7a attenuates post-myocardial infarction remodeling and protects H9c2 cardiomyocytes against hypoxia-induced apoptosis involving Bcl-2. *Cell Physiol Biochem* 2016; 6: 290-298.
- BOUILLET P, METCALE CD, HUANG DC, GIBSON DM, KAY TW, KONTGEN N, STREIBER JM, STRASSER A. Bcl-2 relative to Bcl-xL is required for certain apoptotic responses, leukocyte homeostasis, and to preclude autoimmune disease. *Science* 1999; 286: 1735-1738.
- PURVIS GV, MOULDER KL, CHAMEN JP, BOUILLET P, STREIBER JM, STRASSER A, JOHNSON EM. Induction of a proapoptotic BH3-only BCL-2 family member is critical for neuronal apoptosis. *Neuron* 2000; 26: 615-628.
- WANG Y, LIU X, HUANG H, SUN A, LU C. Involvement of miR-181a in H₂O₂-mediated photodynamically induced apoptosis. *Cell Physiol Biochem* 2015; 35: 1527-1536.
- LIU X, LIU X, ZHANG JJ, FAN W. Involvement of miR-181a and Bim in a rat model of retinal ischemia-reperfusion injury. *Int J Ophthalmol* 2016; 9: 33-40.
- LIU X, CHEN B, CUI F, HE X, WANG W, WANG M. Hypoxia-induced microRNA-301b regulates apoptosis by targeting Bim in lung cancer. *Cell Prolif* 2016; 49: 476-483.
- HUANG C, LI J, HONG K, XIA Z, XU Y, CHENG X. BH3-only protein Bim is upregulated and mediates the apoptosis of cardiomyocytes under glucose and oxygen-deprivation conditions. *Cell Biol Int* 2015; 39: 318-325.
- TAO ZQ, SHI AM, LI R, WANG YQ, WANG X, ZHAO S. Role of microRNA in prostate cancer stem/progenitor cells regulation. *Chin J Integr Med Rev Med Pharmacol Sci* 2016; 20: 3040-3044.
- Katz MG, Fargnoli AS, Kandle A, Galarza RJ, Bridges CR. The role of microRNAs in cardiac development and regenerative capacity. *Physiol Heart Circ Physiol* 2016; 310: H520-H526.
- WANG J, HUANG W, LIU X, NIE Y, LIU X, MENG J, XU X, HU S, ZHENG Z. miR-210-3p regulates cardiac fibrosis after myocardial infarction. *J Cell Mol Med* 2012; 16: 2150-2160.
- LIM S, KIM H, KIM PJ, KIM HT, KIM J, LEE JM, KIM DB, YOO J, CHOI DS, HER SH, YIM J, CHANG K, AHN Y, JEO MH, SHIN BR. Incidence, implications, and predictors of stem cell mobilization in acute myocardial infarction. *Am J Cardiol* 2016; 117: 1562-1568.
- LIU X, FELDMAN BS, LEE J, ROBERTS M, BENIS A. Obesity or smoking: which factor contributes more to the incidence of myocardial infarction? *Eur J Intern Med* 2016; 32: 43-46.
- LIU X, ASTARCI O, MA, ASARCIKL LD, KILIT C, KAFES S, PARSPUR A, CAYMACI M, PINAR M, TUFEKIOGLU O, YILMAZ B. The effects of air pollution and weather conditions on the incidence of acute myocardial infarction. *Am J Emerg Med* 2016; 34: 449-454.
- LIU X, HONMA T, KAKU N. Comparison of incidence, mortality and treatment of acute myocardial infarction in hospitals in Japan and China. *Kurume Med J* 1992; 39: 279-284.
- LUO QO, LONG HB, XU BC. Reduced apoptosis after acute myocardial infarction by simvastatin. *Cell Biochem Biophys* 2015; 71: 735-740.
- MENG Y, LI WZ, SHI YW, ZHOU BF, MA R, LI WP. Danshensu protects against ischemia/reperfusion injury and inhibits the apoptosis of H9c2 cells by reducing the calcium overload through the p-JNK-NF-kappaB-TRPC6 pathway. *Int J Mol Med* 2016; 37: 258-266.
- RENAULT TT, TEJIDO O, ANTONSSON B, DEJEAN LM, MANON S. Regulation of Bax mitochondrial localization by Bcl-2 and Bcl-x(L): keep your friends close but your enemies closer. *Int J Biochem Cell Biol* 2013; 45: 64-67.
- GAO YH, QIAN JY, CHEN ZW, FU MQ, XU JF, XIA Y, DING XF, YANG XD, CAO YY, ZOU YZ, REN J, SUN AJ, GE JB. Suppression of Bim by microRNA-19a may protect cardiomyocytes against hypoxia-induced cell death via autophagy activation. *Toxicol Lett* 2016; 257: 72-83.
- LIU PY, TIAN Y, XU SY. Mediated protective effect of electroacupuncture pretreatment by miR-214 on myocardial ischemia/reperfusion injury. *J Geriatr Cardiol* 2014; 11: 303-310.
- GHOLAMIN S, PASDAR A, KHORRAMI MS, MIRZAEI H, MIRZAEI HR, SALEHI R, FERNS GA, GHAYOUR-MOBARHAN M, AVAN A. The potential for circulating microRNAs in the diagnosis of myocardial infarction: a novel approach to disease diagnosis and treatment. *Curr Pharm Des* 2016; 22: 397-403.

- 24) IZARRA A, MOSCOSO I, LEVENT E, CANON S, CERRADA I, DIEZ-JUAN A, BLANCA V, NUNEZ-GIL IJ, VALIENTE I, RUIZ-SAURI A, SEPULVEDA P, TIBURCY M, ZIMMERMANN WH, BERNAD A. miR-133a enhances the protective capacity of cardiac progenitors cells after myocardial infarction. *Stem Cell Reports* 2014; 3: 1029-1042.
- 25) BHUIYAN MS, TAKADA Y, SHIODA N, MORIGUCHI S, KASAHARA J, FUKUNAGA K. Cardioprotective effect of vanadyl sulfate on ischemia/reperfusion-induced injury in rat heart in vivo is mediated by activation of protein kinase B and induction of FLICE-inhibitory protein. *Cardiovasc Ther* 2008; 26: 10-23.
- 26) HU S, HUANG M, NGUYEN PK, GONG Y, LI Z, LIU J, LIU F, LIU J, NAG D, ROBBINS RC, WU JC. Novel prosurvival cocktail for improving engraftment and function of cardiac progenitor cell transplantation. *Circulation* 2014; 129: S27-34.
- 27) GUO C, DENG Y, LIU J, QIAN L. Myocyte-specific role of miR-24 in promoting cell survival. *J Cell Mol Med* 2015; 19: 103-112.

RETRACTED